

Optimization of a Sandwich Structure Using a Genetic Algorithm

M.R. Khoshravan¹ and M. Hosseinzadeh¹

Abstract: A sandwich panel's optimum core height and composite face thickness, under defined loading, have been computed in order to reach the structure's lowest weight and highest stiffness. The Tsai-Hill criterion was used in order to control the support of transverse loading by the panel. Regarding the relationships in the sandwich materials, the studied material was modeled with the MATLAB package. The Genetic Algorithm (GA) that is based on statistics was used. Our goal was to obtain the best methods of the GA in order to present an optimization method for the sandwich structure. Hence, a sensibility analysis was performed. In conclusion, the influence of the sensibility analysis was found to be useful because it led to a better convergence and decreased the execution time of the problem.

Keywords: Sandwich structure, Genetic algorithm, Optimization, Composite material, Carbon fiber.

1 Introduction

Sandwich structures, such as stratified composites, are composed of two stiff skins that are bonded to both sides of a core by adhesion [See, e.g., Gay, Hoa and Tsai (2003); Pahr and Rammerstorfer (2006); Sharnappa (2007) and Huang and Chiu (2008)]. These materials are largely used in applications that are related to aerospace, automotive, wind station blades and so on. In multilayer stratified composites, the fiber material, number of layers, fiber orientation (0° , $\pm 30^\circ$, $\pm 45^\circ$, $\pm 60^\circ$ and 90°), and lay up sequences are the variables by which the desired mechanical properties are obtained. Since we studied a sandwich panel, the height and core material were added to the parameters. Thus, the design of the sandwich panel required too many parameter combinations. Since these parameters were independent, the use of methods that are based on statistics were highlighted for optimization and design of the sandwich panel [Venkataraman and Haftka (1999)]. Different methods have been suggested in recent years. Zozulya (2009) carried

¹ University of Tabriz, Faculty of Mechanical Engineering, 51666, Tabriz, Iran

out a variational method. Multi-objective methods of optimization were developed [See, e.g. Walker and Smith (2003) and Kipouros, Jaeggi et al. (2008)]. Topology optimization for structural design was performed by several authors [See. e.g. Wang, Lim et al. (2007); Li and Atluri (2008a); Li and Atluri (2008b) and Juan et al. (2008)]. In a contact search in the sliding interface, Oishi and Yoshimura (2008) have combined GA and finite element (FE). As a result, they found approximating polynomials for mapping the local contact search. The optimal value of the weight function's shape parameters for non-uniform grids was presented by Perko and Sarler (2007). Their optimization procedure was set locally on each subdomain. Therefore, each node was optimized separately by the same local reference quality function, according to the specific node distribution. A two-dimensional boundary element formulation has been presented by de Lacerda and da Silva (2006) and coupled to a genetic algorithm in order to identify the polarization curves of the buried slender structures. The dual boundary element method was implemented in order to model cathodic protection of the metallic body and the genetic algorithm was employed to deal with the inverse problem of determining the non-linear polarization curve. Aymerich and Serra (2006) explored the potential of the Ant Colony Optimization (ACO) metaheuristic for the optimization of stacking sequences in composite laminates. For both unconstrained and constrained optimization lay-up problems, the analyses indicated that the proposed ACO algorithm is able to achieve reasonably good solutions within very few iterations and extremely high quality solutions within a limited number of runs, with respect to the total number of possible solutions.

Of the available optimization methods, GA has been the most useful in recent years [See, e.g. Narayana, Gopalakrishnan and Ganguli (2008) and Sinha and Ch. (2008)]. Using the genetic algorithm (GA), we wanted to obtain the lowest thickness of the composite faces and the lowest height of the structure that would therefore give the lowest weight to support a given transverse load. A number of methods that employ the GA to optimize the sandwich structures have been identified in the literature in recent years. The most important findings that correspond with our research are explained in the following. The weight of a composite structure and the orientation of its fibers have been optimized using a multi-objective optimization method and the GA that were combined using the FE method [Walker and Smith (2003)]. The optimization of the sandwich structure's core and fiber-reinforced skins, which are used in the panels, have been analyzed by minimizing the weight of the structure and the fiber reinforced polymer (FRP) skins. In the optimization, combinations of continuous and discrete variables that correspond to the geometrical and material parameters have been used. The GA analyzed these variables well, even though they were sometimes put close together in a non-standard

manner [He and Aref (2003)]. The lay up sequence of the composite layers of the sandwich structure’s skins was optimized using the FE method. In the experimental part, several stratified sandwiches were loaded with a transverse charge and the resistance limit of the sandwich sheets was evaluated. Then, using the FE method, the weight of the sheets was optimized in two steps. Simple supports and cantilever supports were used. The load was applied in both a concentrated and distributed form. The orientation of the fibers was 0°, 45° and 90°. The Tsai-Wu criterion was used as the failure criterion [Kam, Lai, and Chao (1999)]. Other novel methods in the optimization of the mechanical behavior of sandwich structures, such as multi-objective optimization for the prismatic core, were developed [Tan and Soh (2007)].

In conclusion, the optimum design of composites would be devised into three parts: modeling, treatment of the model and optimization. Each one could be considered to be simple or complicated. The complication would lead to a high precision but would increase the time and cost of the treatment.

2 Governing equations

2.1 Mechanical behavior of the composite skins

By choosing an adequate lay up sequence for the skins, we can choose the desired properties of the composite and optimize the composite material’s mechanical behavior, which is either the low weight or high stiffness. As an example, a composite with N layers, for the layer situated in the K position, Hook’s law is shown in Eq. (1) [Vinson (1997)].

$$\begin{pmatrix} \sigma_x \\ \sigma_y \\ \sigma_z \\ \sigma_{yz} \\ \sigma_{xz} \\ \sigma_{xy} \end{pmatrix} = \begin{bmatrix} \bar{Q}_{11} & \bar{Q}_{12} & \bar{Q}_{13} & 0 & 0 & 2\bar{Q}_{16} \\ \bar{Q}_{12} & \bar{Q}_{22} & \bar{Q}_{23} & 0 & 0 & 2\bar{Q}_{26} \\ \bar{Q}_{13} & \bar{Q}_{23} & \bar{Q}_{33} & 0 & 0 & 2\bar{Q}_{36} \\ 0 & 0 & 0 & 2\bar{Q}_{44} & 2\bar{Q}_{45} & 0 \\ 0 & 0 & 0 & 2\bar{Q}_{45} & 2\bar{Q}_{55} & 0 \\ \bar{Q}_{16} & \bar{Q}_{26} & \bar{Q}_{36} & 0 & 0 & 2\bar{Q}_{66} \end{bmatrix} \begin{pmatrix} \epsilon_x \\ \epsilon_y \\ \epsilon_z \\ \epsilon_{yz} \\ \epsilon_{xz} \\ \epsilon_{xy} \end{pmatrix} \quad (1)$$

By considering the relationships between the stress and strain in orthotropic materials, the elements of matrix \bar{Q} were obtained as presented in Eq. (2) [Vinson

(1997)].

$$\begin{aligned}
 \bar{Q}_{11} &= Q_{11}m^4 + 2(Q_{12} + 2Q_{66})m^2n^2 + Q_{22}n^4 \\
 \bar{Q}_{12} &= (Q_{11} + Q_{22} - 4Q_{66})m^2n^2 + Q_{12}(m^4 + n^4) \\
 \bar{Q}_{13} &= Q_{13}m^2 + Q_{23}n^2 \quad \bar{Q}_{33} = Q_{33} \\
 \bar{Q}_{16} &= -mn^3Q_{22} + m^3nQ_{11} - mn(m^2 - n^2)(Q_{12} + 2Q_{66}) \\
 \bar{Q}_{22} &= Q_{22}m^4 + 2(Q_{12} + 2Q_{66})m^2n^2 + Q_{11}n^4 \\
 \bar{Q}_{23} &= n^2Q_{13} + m^2Q_{23} \quad \bar{Q}_{36} = (Q_{13} - Q_{23})mn \\
 \bar{Q}_{26} &= mn^3Q_{11} - m^3nQ_{22} - mn(m^2 - n^2)(Q_{12} + 2Q_{66}) \\
 \bar{Q}_{44} &= n^2Q_{55} + m^2Q_{44} \quad \bar{Q}_{45} = (Q_{55} - Q_{44})mn \\
 \bar{Q}_{36} &= (Q_{13} - Q_{23})mn \quad \bar{Q}_{55} = n^2Q_{44} + m^2Q_{55} \\
 \bar{Q}_{66} &= (Q_{11} + Q_{22} - 2Q_{12})m^2n^2 + Q_{66}(m^2 - n^2)^2
 \end{aligned} \tag{2}$$

The displacements of the sheet are presented in Eq. (3) by choosing a rectangular element with a low thickness, h , from the composite laminate and by considering the x - y coordinates to be in the middle plane while the z coordinate is normal to the middle plane [Kant and Swaminathan (2002)].

$$\begin{aligned}
 u(x, y, z) &= u_{\bullet}(x, y) + z\bar{\alpha}(x, y) \\
 v(x, y, z) &= v_{\circ}(x, y) + z\bar{\beta}(x, y) \\
 w(x, y, z) &= w_{\circ}(x, y) \\
 \bar{\alpha} &= -\partial w / \partial x, \quad \bar{\beta} = -\partial w / \partial y
 \end{aligned} \tag{3}$$

u_{\bullet} , v_{\circ} and w_{\circ} are the displacements of the middle plane. In the classical theory of plates and beams, $\bar{\alpha}$ and $\bar{\beta}$ are equal to the negative first derivate of the transverse displacement relative to the x - y coordinates. In the same theory, the displacement in the z direction is considered to be independent of the layer's torsion; thus, $w=w(x,y)$. By substitution of the strain relations in Eq. (3), we obtained the relations of Eq. (4):

$$\begin{aligned}
 \epsilon_x &= \frac{\partial u_{\circ}}{\partial x} + z\frac{\partial \bar{\alpha}}{\partial x}, \quad \epsilon_y = \frac{\partial v_{\circ}}{\partial y} + z\frac{\partial \bar{\beta}}{\partial y}, \quad \epsilon_z = 0 \\
 \epsilon_{xz} &= \frac{1}{2}(\bar{\alpha} + \frac{\partial w}{\partial x}), \quad \epsilon_{yz} = \frac{1}{2}(\bar{\beta} + \frac{\partial w}{\partial y}) \\
 \epsilon_{xy} &= \frac{1}{2}(\frac{\partial u_{\circ}}{\partial y} + \frac{\partial v_{\circ}}{\partial x}) + \frac{1}{2}(\frac{\partial \bar{\alpha}}{\partial y} + \frac{\partial \bar{\beta}}{\partial x})
 \end{aligned} \tag{4}$$

In the theory of plates, each layer has its own strain and displacement. The conti-

nuity of the strain and displacement is independent of the orientation of each layer.

$$\begin{Bmatrix} \sigma_x \\ \sigma_y \\ \sigma_{yz} \\ \sigma_{xz} \\ \sigma_{xy} \end{Bmatrix}_{[k]} = [\bar{Q}]_k \begin{Bmatrix} \epsilon_{x_0} + z \frac{\partial \bar{\alpha}}{\partial x} \\ \epsilon_{y_0} + z \frac{\partial \bar{\beta}}{\partial y} \\ \epsilon_{yz} \\ \epsilon_{xz} \\ \epsilon_{xy_0} + \frac{z}{2} \left(\frac{\partial \bar{\alpha}}{\partial y} + \frac{\partial \bar{\beta}}{\partial x} \right) \end{Bmatrix}_k \tag{5}$$

Due to the negligible thickness of the layer, ϵ_z is considered null. Thus, for a thin-walled composite, σ_z is not usually taken into consideration. Since the variations are considered continuous and linear, we could consider the strain matrix of Eq. (5) without the subscript K in all of the layers. But due to the different orientation in the layers, the stress does not have a continuous state and the subscript K should remain. Regarding Fig. 1, the middle plane is the reference, so $Z=0$ and h_k is the distance of the K^{th} layer from the middle plane. This value is positive for the upper layers of the middle plane and negative for the lower layers.

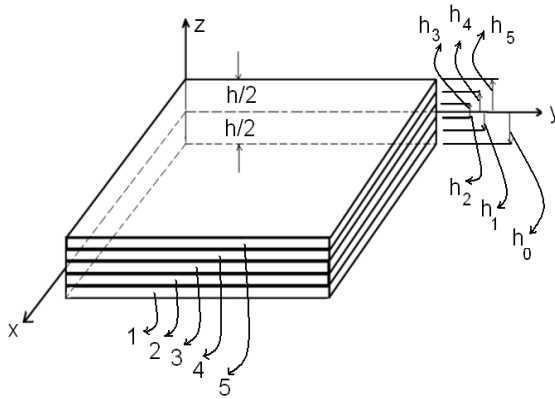


Figure 1: The height and position of each layer with respect to the middle plane of the laminate [Park, Hawang, Lee and Hwang (2001)]

Following the classic theory of plates and shells, the normal load (N), moment (M) and shear load (Q) that resulted from the stresses are given by Eq. (6). This definition is independent of the number of layers and their orientation in the laminate

[Vinson and Sierakowski (1987)].

$$\begin{Bmatrix} N_x \\ N_y \\ N_{xy} \\ Q_x \\ Q_y \end{Bmatrix} = \int_{-h/2}^{+h/2} \begin{Bmatrix} \sigma_x \\ \sigma_y \\ \sigma_{xy} \\ \sigma_{xz} \\ \sigma_{yz} \end{Bmatrix} dz, \quad \begin{Bmatrix} M_x \\ M_y \\ M_{xy} \end{Bmatrix} = \int_{-h/2}^{+h/2} \begin{Bmatrix} \sigma_x \\ \sigma_y \\ \sigma_{xy} \end{Bmatrix} z dz \tag{6}$$

2.2 Equilibrium equations

We first modeled the laminates by analyzing the equilibrium equations. An element with the properties of the material was chosen. The stresses at the boundaries and the components of the body load (F_x, F_y and F_z) have also been applied to the whole element. The equilibrium equations in three principal directions are presented in Eq. (7).

$$\begin{aligned} \frac{\partial \sigma_x}{\partial x} + \frac{\partial \sigma_{yx}}{\partial y} + \frac{\partial \sigma_{zx}}{\partial z} + F_x &= 0 \\ \frac{\partial \sigma_{xy}}{\partial x} + \frac{\partial \sigma_y}{\partial y} + \frac{\partial \sigma_{zy}}{\partial z} + F_y &= 0 \\ \frac{\partial \sigma_{xz}}{\partial x} + \frac{\partial \sigma_{yz}}{\partial y} + \frac{\partial \sigma_z}{\partial z} + F_z &= 0 \end{aligned} \tag{7}$$

In the composite sheets, with the low thickness, the integral of the stresses in the thickness of the sheet was found. By doing this work on the equilibrium equations and by neglecting the body loads, Eq. (8) was obtained [Altnbach, H. and Altnbach, J. (2004)]:

$$\begin{aligned} \frac{\partial N_x}{\partial x} + \frac{\partial N_{yx}}{\partial y} + \tau_{1x} - \tau_{2x} &= 0 \\ \frac{\partial N_{xy}}{\partial x} + \frac{\partial N_y}{\partial y} + \tau_{1y} - \tau_{2y} &= 0 \\ \frac{\partial Q_x}{\partial x} + \frac{\partial Q_y}{\partial y} + p_1 - p_2 &= 0 \end{aligned} \tag{8}$$

Except the above relations, the two moment equilibrium relations in the x and y directions were necessary. By crossing the two equilibrium equations of the x and y directions in zdz and by integrating through the width of the laminate, Eq. (9) was obtained:

$$\begin{aligned} \frac{\partial M_x}{\partial x} + \frac{\partial M_{xy}}{\partial y} - Q_x + \frac{h}{2}[\tau_{1x} + \tau_{2x}] &= 0 \\ \frac{\partial M_{xy}}{\partial x} + \frac{\partial M_y}{\partial y} - Q_y + \frac{h}{2}[\tau_{1y} + \tau_{2y}] &= 0 \end{aligned} \tag{9}$$

2.3 Theory of the minimal potential energy

For an elastic material, the potential energy of the body is as presented in Eq. (10) [Vinson (1999)]:

$$V = \int_R W_u dR - \int_{S_r} T_i U_i ds - \int_R F_i U_i dR \quad (10)$$

The theory of minimum potential energy expresses that from all of the possible displacements, which are compatible with the studied problem and respect the boundary conditions, those who respect the equilibrium equations minimize the potential energy function. Using the minimum potential energy, the stresses were converted to strains from the stress-strain relations and the strains were converted to displacements from the strain-displacement relations. Then, using the theory of the minimum potential energy in a composite sheet, Eq. (11) was obtained [Vinson and Sierakowski (1987)].

$$V = \frac{1}{2} \sum_{k=1}^N \int \int_A \int_{h_{k-1}}^{h_k} \{ \sigma_x \epsilon_x + \sigma_y \epsilon_y + 2\sigma_{xz} \epsilon_{xz} + 2\sigma_{yz} \epsilon_{yz} \} dz dA - \int \int P(x,y) w(x,y) dA \quad (11)$$

By substituting the stress-strain equations and the strain-displacement relations into Eq. (11) and then considering the middle plane's symmetry in the composite skins, Eq. (12) has been obtained. The middle plane's symmetry in the composite lami-

nates is explained by Gay, Hoa, and Tsai (2003).

$$\begin{aligned}
 V = \int \int_A \left\{ \frac{A_{11}}{2} \left(\frac{\partial u_0}{\partial x} \right)^2 + B_{11} \frac{\partial u_0}{\partial x} \cdot \frac{\partial \bar{\alpha}}{\partial x} + \frac{D_{11}}{2} \left(\frac{\partial \bar{\alpha}}{\partial x} \right)^2 + A_{12} \frac{\partial u_0}{\partial x} \cdot \frac{\partial v_0}{\partial y} \right. \\
 + B_{12} \left[\frac{\partial u_0}{\partial x} \cdot \frac{\partial \bar{\beta}}{\partial y} + \frac{\partial u_0}{\partial y} \cdot \frac{\partial \bar{\alpha}}{\partial x} \right] \\
 + D_{12} \frac{\partial \bar{\beta}}{\partial y} \cdot \frac{\partial \bar{\alpha}}{\partial x} + A_{16} \left[\frac{\partial u_0}{\partial x} \frac{\partial v_0}{\partial y} + \frac{\partial u_0}{\partial x} \frac{\partial v_0}{\partial x} \right] + D_{16} \left[\frac{\partial \bar{\alpha}}{\partial x} \frac{\partial \bar{\alpha}}{\partial y} + \frac{\partial \bar{\alpha}}{\partial x} \frac{\partial \bar{\beta}}{\partial x} \right] \\
 + B_{16} \left[\frac{\partial u_0}{\partial x} \frac{\partial \bar{\alpha}}{\partial y} + \frac{\partial u_0}{\partial x} \frac{\partial \bar{\beta}}{\partial x} + \frac{\partial u_0}{\partial y} \frac{\partial \bar{\alpha}}{\partial x} + \frac{\partial v_0}{\partial x} \frac{\partial \bar{\alpha}}{\partial x} \right] + \frac{A_{22}}{2} \left(\frac{\partial v_0}{\partial y} \right)^2 \\
 + B_{22} \frac{\partial v_0}{\partial y} \cdot \frac{\partial \bar{\beta}}{\partial y} + \frac{D_{22}}{2} \left(\frac{\partial \bar{\beta}}{\partial y} \right)^2 \\
 + A_{26} \left[\frac{\partial v_0}{\partial y} \frac{\partial u_0}{\partial y} + \frac{\partial v_0}{\partial y} \frac{\partial v_0}{\partial x} \right] + B_{26} \left[\frac{\partial u_0}{\partial x} \frac{\partial \bar{\alpha}}{\partial y} + \frac{\partial v_0}{\partial y} \frac{\partial \bar{\beta}}{\partial x} + \frac{\partial u_0}{\partial y} \frac{\partial \bar{\beta}}{\partial y} + \frac{\partial v_0}{\partial x} \frac{\partial \bar{\beta}}{\partial y} \right] \\
 + D_{26} \left[\frac{\partial \bar{\alpha}}{\partial y} \frac{\partial \bar{\beta}}{\partial y} + \frac{\partial \bar{\beta}}{\partial x} \frac{\partial \bar{\beta}}{\partial y} \right] + A_{45} \left[\bar{\alpha} \bar{\beta} + \bar{\alpha} \frac{\partial w}{\partial y} + \bar{\beta} \frac{\partial w}{\partial x} + \frac{\partial w}{\partial y} \frac{\partial w}{\partial x} \right] \\
 + A_{55} \left[\frac{\bar{\alpha}^2}{2} + \bar{\alpha} \frac{\partial w}{\partial x} + \frac{1}{2} \left(\frac{\partial w}{\partial x} \right)^2 \right] + A_{44} \left[\frac{\bar{\beta}^2}{2} + \bar{\beta} \frac{\partial w}{\partial x} + \frac{1}{2} \left(\frac{\partial w}{\partial y} \right)^2 \right] \\
 + A_{66} \left[\frac{1}{2} \left(\frac{\partial u_0}{\partial y} \right)^2 + \frac{\partial u_0}{\partial y} \frac{\partial v_0}{\partial x} + \frac{1}{2} \frac{\partial v_0}{\partial y} \left(\frac{\partial v_0}{\partial x} \right)^2 \right] \\
 + B_{66} \left[\frac{\partial u_0}{\partial y} \frac{\partial \bar{\alpha}}{\partial y} + \frac{\partial u_0}{\partial y} \frac{\partial \bar{\beta}}{\partial x} + \frac{\partial v_0}{\partial x} \frac{\partial \bar{\alpha}}{\partial y} + \frac{\partial v_0}{\partial x} \frac{\partial \bar{\beta}}{\partial x} \right] \\
 \left. + D_{66} \left[\frac{1}{2} \left(\frac{\partial \bar{\alpha}}{\partial y} \right)^2 + \frac{\partial \bar{\alpha}}{\partial y} \frac{\partial \bar{\beta}}{\partial x} + \frac{1}{2} \left(\frac{\partial \bar{\beta}}{\partial x} \right)^2 \right] - P(x,y)w(x,y) \right\} dA
 \end{aligned}
 \tag{12}$$

To resolve Eq. (12), the Rilly-Ritz method was used. In this method, an initial guess for the form of the deflection function was assumed. This initial proposition should respect the boundary conditions (B.C.). In this research, the B.C. was chosen to be the base of four simple supports. Thus, using the equations of Vinson (1999) for the above mentioned B.C., the functions that are illustrated by Eq. (13) were

considered:

$$\begin{aligned}
 w(x, y) &= \sum_{m=1}^{\infty} \sum_{n=1}^{\infty} W_{mn} \sin \lambda_m x \sin \lambda_n y \\
 \bar{\alpha}(x, y) &= \sum_{m=1}^{\infty} \sum_{n=1}^{\infty} \Gamma_{mn} \sin \lambda_m x \cos \lambda_n y \\
 \bar{\beta}(x, y) &= \sum_{m=1}^{\infty} \sum_{n=1}^{\infty} \Lambda_{mn} \cos \lambda_m x \sin \lambda_n y \\
 u_0(x, y) &= \sum_{m=1}^{\infty} \sum_{n=1}^{\infty} U_{mn} \sin \lambda_m x \cos \lambda_n y \\
 v_0(x, y) &= \sum_{m=1}^{\infty} \sum_{n=1}^{\infty} V_{mn} \cos \lambda_m x \sin \lambda_n y
 \end{aligned} \tag{13}$$

Based on the Rilly-Ritz method, in the minimum potential energy principle, the expression of v was derived relative to the unknown amplitudes of Eq. (7) and was taken as zero. Thus, a system of 20 equations with 20 unknowns was obtained. By resolving that system, the unknown amplitudes were obtained and the deflection and rotation functions were known. Then, by knowing the deflection and displacement, the strains of Eq. (4) were obtained from the strain-displacement relations and used to compute the stresses of Eq. (1).

2.4 Failure criterions

There are many failure criteria for orthotropic materials. The criterion most commonly used for design calculations is the Hill-Tsai criterion [Gay, Hoa, and Tsai (2003)] illustrated in Eq. (14).

$$\left(\frac{\sigma_1}{x}\right)^2 + \left(\frac{\sigma_2}{y}\right)^2 - \frac{\sigma_1 \sigma_2}{x^2} + \left(\frac{\sigma_{12}}{S}\right)^2 \leq 1 \tag{14}$$

With regards to the core that is made of foam, the maximum shear stress criterion was applied since it supports only the shear load.

3 Optimization

The genetic algorithm is one of the most complete methods of optimization [Gen and Cheng (2000)]. Genetic science consists of the transfer of biological characteristics, such chromosomes and genes. Following this science, the strongest genes and chromosomes remain by destroying the weakest ones. The application of GAs for optimization requires the definition of three points:

1. Objective function or Cost function
2. Genetic representation
3. GA operators.

If these three points are well-defined, the GA functions correctly. If necessary, some corrections can be applied.

3.1 Objective function

The objective of this research was to decrease the number of layers of skin and to decrease the height of the core, while at the same time allowing the sandwich structure to support the applied load. To reach both of the goals, we chose an objective function in order to minimize the weight of the sandwich structure. Thus, the objective function should indicate the weight of the structure. Eq. (15) has been chosen as the objective function.

$$W = \sum_{k=1}^n \rho_1 h_k + h \rho_2 \quad (15)$$

In this relation, n is the number of layers of skins. h_k is the thickness of each layer and it is equal to $0/125.10^{-3}$ m for all of the laminates. ρ_1 and ρ_2 are, respectively, the density of the skins and the core while h is the height of the core. To define the fitness, the individuals in the population were ranked relative to their weight. The lightest person had the number 1 and the heaviest person had the number N_{pop} (the last person in the population).

3.2 Genetic representation

In order to optimize the sandwich structure, synchronization variables had to be chosen. The variables were the number of layers in the composite laminate skins, the orientation of the fibers in each layer, the composite laminate material, the foam material that constitutes the core and the thickness. Thus, the chromosome needed to include 13 genes. The first gene related to the laminate material (one character). The second gene related to the foam material (two characters). The next ten genes defined each laminate's fiber orientation (three characters) and the last gene that contains six characters defined the thickness of the foam. These genes are explained in Section 4.2. Thus, the shape of the chromosome is illustrated in Fig.2.

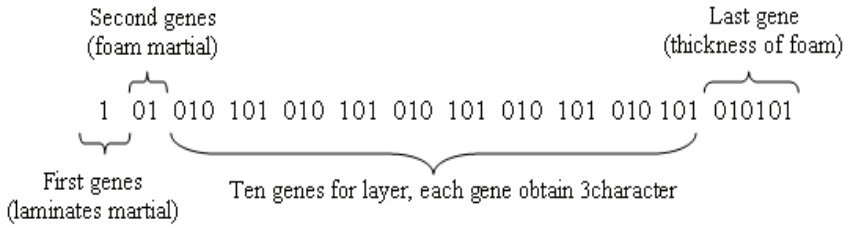


Figure 2: The shape of the chromosome

3.3 Genetic algorithm operators (GA)

All of the steps in the application of the GA to an optimization problem are explained in the literature [See, e.g., Venkataraman and Haftka (1999); Gen and Cheng (2000) and Haupt R.L., Haupt (2004)].

Generally, in a GA, three inheritance operators are used:

- 1- Reproduction
- 2- Crossover
- 3- Mutation.

In order to prevent large scatter in the responses and to obtain a uniform responses, we applied the scale factor method to the chromosomes. The different methods that were used for the scale factor were:

- 1- Rank
- 2- Top
- 3- Uniform.

Different methods were used to choose the chromosomes and to cross them over. The most important were described by Rajasekaran and Vijayalakshmpai (2005):

- 1- Roulette wheel method
- 2- Tournament method
- 3- Uniform method.

The different crossover operator methods was:

- 1- Single-point crossover
- 2- Two-point crossover
- 3- Uniform crossover

3.4 Error function

As mentioned, we wanted to decrease the weight of the stratified sandwich by decreasing the number of skin layers and also by decreasing the height of the core. For these conditions to ensure that the sandwich structure would be tough enough to support the applied load, the Hill-Tsai criterion was used. The difference between the tensile and compressive strength in the Tsai-Hill rule was taken into consideration.

If, in a chromosome, the number of layers was too low to support the applied load or if the shear stress was high enough to destroy the core, the failure criterions would identify this chromosome. Thus, the probability of transferring this chromosome to the next generation would decrease significantly.

4 Hypothesis of the problem

4.1 Device

The load was statically distributed across the width direction of the sheet. The sheet has a square shape and is put on simple supports. It is symmetric relative to its middle plane. The angles of the reinforcing fibers in the composite skins were chosen between 0° , $\pm 30^\circ$, $\pm 45^\circ$, $\pm 60^\circ$ and 90° . Thus, the parameter of each layer is its fiber orientation. The thicknesses of all of the layers of skins in the composite laminate were similar. We compared our results with the existing most similar experimental results of Kam, Lai and Chao (1999). The type of loading and the details of the sandwich panel are illustrated in Fig. 3, which was taken from the same reference.

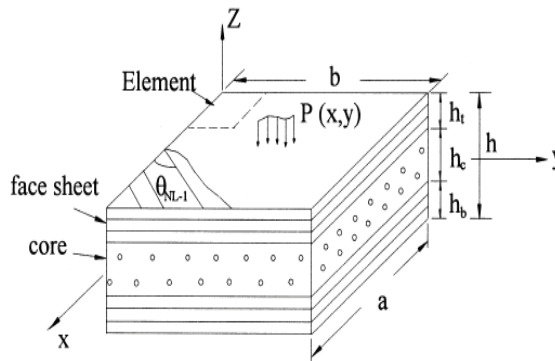


Figure 3: The sandwich panel and its loading [Kam, Lai and Chao (1999)]

4.2 Material

4.2.1 Laminate composite of the skins

Two composite materials were chosen for the skins. The first one was a T50/1962 Carbon/Epoxy and the second was a T300-5208 Carbon/Epoxy. In the GA, the gene that corresponds to the first material in the skin was represented by zero and the second by one. Their mechanical properties are in Tab. 1.

In Tab. 1, E is the Young's modulus, G is the shear stress and ν is Poisson's ratio. The subscripts one, two, and three correspond, respectively, to the x , y and z axes, as per Fig. 3. X and X' are the rupture stresses in the x -axis direction in tension and compression, respectively. Y and Y' are the rupture stresses in the y -axis direction

Table 1: Properties of the skins [Peters (1998)].

	E ₁₁ GPa	E ₂₂ E ₃₃ GPa	G ₁₂ GPa	G ₂₃ GPa	v ₁₂	v ₂₃ v ₁₃	X MPa	X' MPa	Y MPa	Y' MPa	S MPa	ρ Kg/ m ³
T50	241	7	6	3	0.28	0.35	1431	965	37	159	63	1720
T300	181	10.3	7.2	3.36	0.28	0.3	1500	1500	40	260	68	1600

in tension and compression, respectively. S is the shear rupture stress and ρ is the density.

Each skin was made of a composite laminate that contains 20 layers that are symmetrically situated relative to their middle plane. Thus, the GA required 10 genes to be defined for each skin. We decided to choose the orientation of each layer between the angles of $0^\circ/\pm 30^\circ/\pm 45^\circ/\pm 60^\circ/90^\circ$. As there are eight different orientations that follow the binary notation, each of the above mentioned orientations was presented by a gene that contains three characters.

4.2.2 Core and its height

The core of the sandwich was made of foam. Four different foams were studied. Table 2 shows their mechanical properties.

Table 2: Properties of the core [Hyer (1998)]

	Polyester	Epoxy	Bismaleimide	Vinyl ester
Density (Kg/m ³)	1300	1250	1320	1150
Tensile modulus (GPa)	2.85	4	3.6	3.5
Tensile resistance (MPa)	65	85.5	63	77.5

In Tab. 2, the materials from left to right were numbered one to four. Hence, in the GA, the second gene that corresponds to the materials of the core was presented by a gene that contains two characters.

The height of the core was variable. The maximum and minimum chosen values were $hc_{max} = 0.04$ mm and $hc_{min} = 0.002$ mm. In the GA, a gene with six characters

was chosen. It represents 64 combinations, which is a large bound of values for the height in the mentioned domain.

4.3 Evaluation of the validity of the results

An algorithm was written with MATLAB software in order to evaluate the validity of the results that were obtained from the existing relations between the stratified sandwich, the different GA operators and the failure criteria (Fig.4).

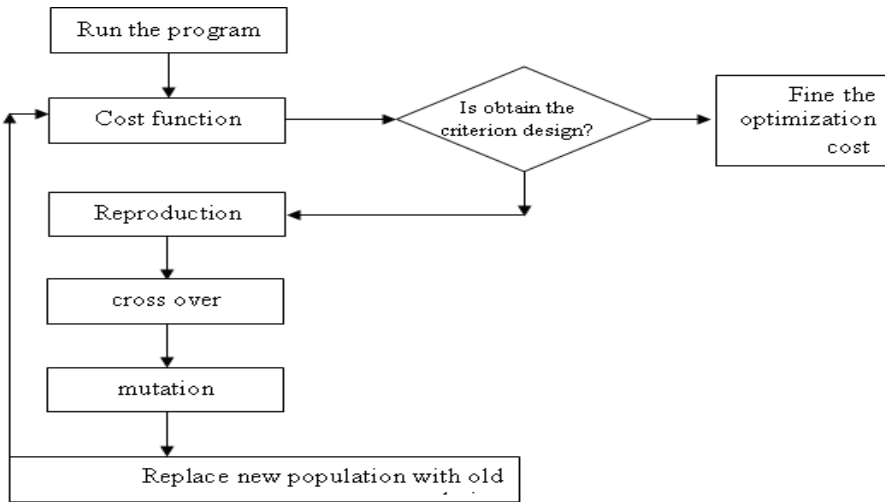


Figure 4: Flow chart of the GA for evaluation of the results' validity

We had to check how many results were correct and if we could have confidence in this algorithm. For this reason, first we compared our results with those of Kam, Lai, and Chao, (1999) as mentioned in Section 4.1, and then we controlled the precision of the GA with the test function.

5 Results and discussion

The results of the sandwich layers that were optimized with the GA and the finite element are illustrated in Table (3). As presented in Table 3, the results are similar to each other.

5.1 Precision of the results

After being ensured of the validity of the results, we analyzed the precision of the results. For this purpose, we used a function for which we knew the exact position

Table 3: Comparison of the results of the FE with the GA

	<i>First step</i>		<i>Second step</i>		<i>Third step</i>	
	Orientation, height	Weight (g)	Orientation, height	Weigh (g)	Orientation, height	Weight (g)
FE	[45 ₂ /-45 ₃₂] _s 0.751 cm	188.07	[45 ₁ /-45 ₁ /45 ₃₁] _s 0.761 cm	184.26	[45 ₁ /-45 ₁ /45 ₁ /-45 ₂₉] _s 0.778 cm	180.82
GA	[±60 ₂ /0 ₆ /±45/±30 ₂] _s 0.98 cm	191.2	[±60 ₂ /0 ₂ /±45/30/90 ₄] _s 0.83 cm	188.3	[±60 ₂ /0 ₂ /±45 ₂ /±30/90 ₂] _s 0.79 cm	180.04

of its minimum and maximum points. We presented it to the GA as the cost function and we analyzed its answers. The function that was used for testing of the algorithm is presented by Eq. (16).

$$z = (x^2 + y^2)^{0.25} * \sin \left\{ 30 [(x + .5)^2 + y^2]^{0.1} \right\} + |x| + |y| \tag{16}$$

The global view of Eq. (16) that was used as the cost function for testing has been illustrated in Fig. 5.

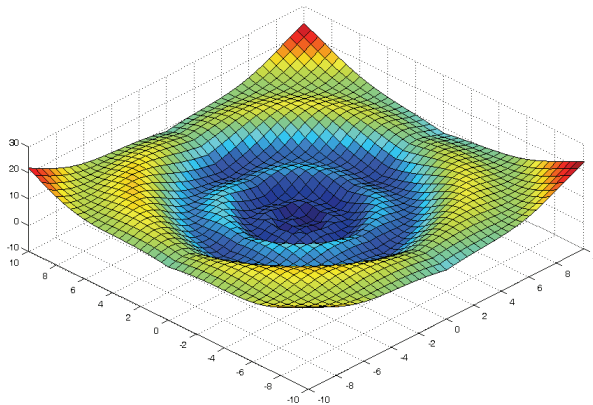


Figure 5: Global view of the cost function for testing

The function had many local minima but it only had one absolute minimum that was situated at the coordinate (0,0). The best answer that was obtained by the GA for that function was in the 50th generation.

5.2 Convention

To compare the different methods, all of the results were illustrated with different curves. The method that was used was indicated in each curve in order to make a correct comparison. As there are a large number of parameters, each one was presented by its special symbol in the above, right side of the figure, according to Tab. 4. The (?) symbol means that the corresponding symbol has not been taken into account.

Table 4: Symbols of the different parameters

<i>Operator</i>	<i>Method</i>	<i>Symbol</i>	<i>Operator</i>	<i>Method</i>	<i>Symbol</i>
Scale function	Rank	F1	Selection	Roulette	S1
	Top	F2		Tournament	S2
	Uniform	F3		Uniform	S3
Crossover	Single-point	C1	Mutation	Uniform	M1
	Two-point	C2		Delete	M2
	Scattered	C3			
Population size		P...	Generation size		I ...
Crossover rate		Cr ...	Mutation rate		Mr ...

5.3 Sensibility analysis

After ensuring that the GA was functional, we had to optimize its operating manner. The successful execution of the GA depended on the right choice of its operators, such as the population size, crossover, mutation, generation size, selection method, child production, and so on. Thus, the sensibility analysis was used to optimize the GA's operators.

The best state of each operator was obtained by trial and error by keeping the other operators constant. In our analysis, we chose three operators for the scale factor, three operators for the selection method, three operators for the crossover, and two operators for the mutation. Before choosing the operators, the population size, generation size, crossover rate, and method of mutation were determined.

5.4 Results of the GA methods

5.4.1 Crossover rate

The crossover rate determines the quantity of parents that enter into the mating pool. If the quantity is high, the opportunity to integrate chromosomes would be lost. If the quantity is low, the quantity of produced children would not be sufficient. Thus, the optimized quantity of parents should be determined. It is a number from zero to one. To obtain the best coefficient by its variation and by keeping the other variables constant, variations in the crossover rate were studied.

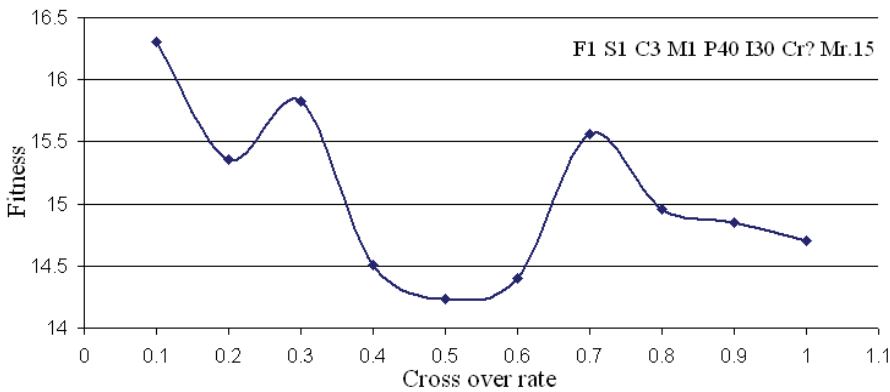


Figure 6: Obtaining the best crossover rate coefficient

From Fig. 6, the crossover rate has its lowest fitness (the lowest weight that the structure could have) at 0.5. It is noted that this curve was obtained by the cited methods.

5.4.2 Population size

The population size was chosen to correctly cover the search area and also to keep the execution speed of the algorithm good.

We observed that we had not obtained similar final responses with different methods. Normally, an increase in the population size should give a better response. In fact, the type of method was different and, since the subject of each method had its own special property, each of the methods had their own manner of resolving the problem. Thus, not all of the methods gave similar responses regarding the cost function, quantity of chromosomes, and number of genes, which we defined in our research. Some of methods gave a good response for the short chromosomes but a higher population and generation size was needed for long chromosomes. Another

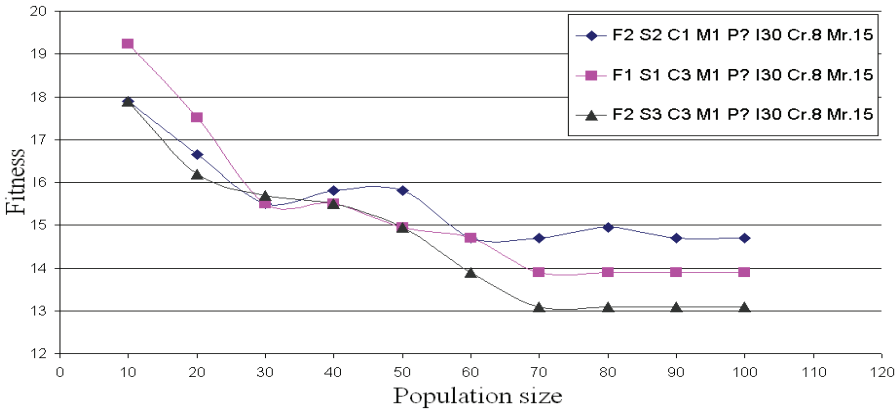


Figure 7: Obtaining a convenient population size using different methods

cause of the difference in fitness quantity was the relationship between the methods. Some of the methods had a good relationship with the other methods and were eliminated by mutual default. On the other hand, some of methods increased the defaults of each other.

Fig. 7 shows that when the population size reached 70, there was not a significant change of fitness for each of the three methods and the fitness reached its minimum value. Thus, a population size between 60 and 70 would be acceptable.

5.4.3 Generation size

Increasing the generation size led to better final results but it increased the time of the program's execution. Fig. 8 illustrates the influence of increasing the population size. We observed that by increasing the population size, we reached the final state in a low generation size.

In the section on population size (5.4.2.), the best population size for different methods was 70. Also, in the section on generation size, a population size of 70 reached the final result first. If we should suggest a generation size for each of the populations, a generation size of 100 would be acceptable for all methods.

5.4.4 Mutation

The mutation operator contains two methods. The first one, which should exist in all of the cases, is called "uniform" while the second method called "delete" is only for the elimination of the layers. Its principal role was to help the convergence. This operator could be eliminated if necessary.

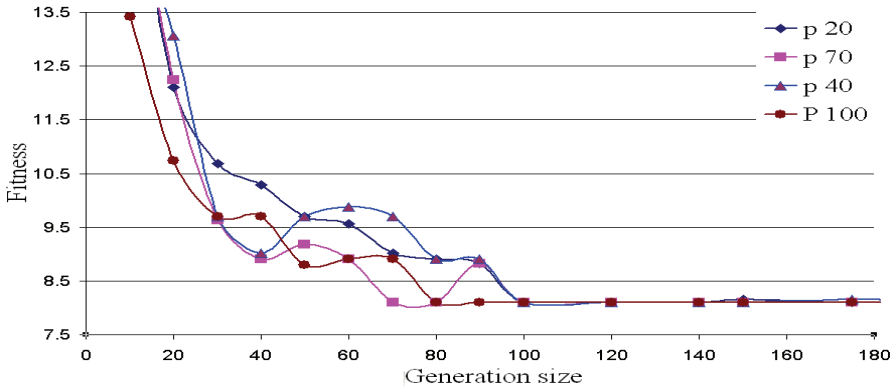


Figure 8: Obtaining a convenient generation for different population sizes

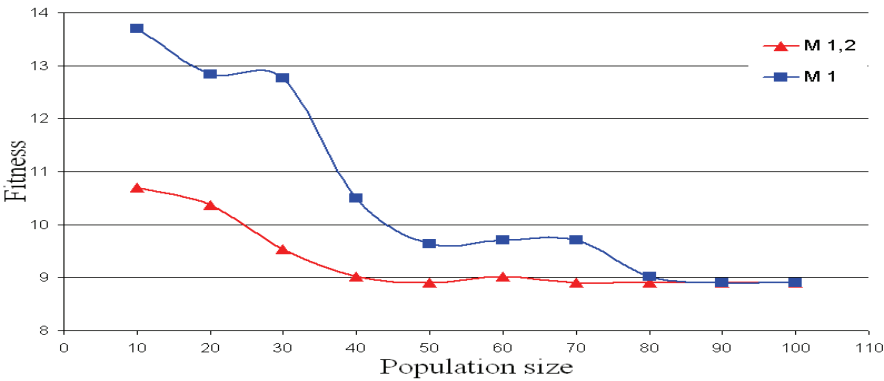


Figure 9: Comparing the M1 and M1,2 states

As Fig.9 illustrates, M1,2 contains both the uniform and delete methods and reached, for the first time, the final result with a population size of 50; whereas, M1 reached this value with a population size of 90. Thus, we concluded that the M1,2 method would cause the convergence speed to increase.

5.4.5 Mutation rate

Fig.10 shows that the “uniform” mutation method, only by itself and without the "delete" method, was not able to find a convenient number by varying the mutation rate from 0.05 to 0.5. This can be explained as follows; the length of the chromosome is too high (39 characters) and the mutation rate, which is at its maximum value (0.5), could only change 58 characters for all of the population sizes that

should be created by the mutation. Thus, each chromosome could perform about ten changes. Since 30 characters of each chromosome concern the fiber orientation and orientation changes that did not change the weight of the structure, we concluded that the “uniform” mutation method, regarding the type of chromosome and the type of cost function, was not useful.

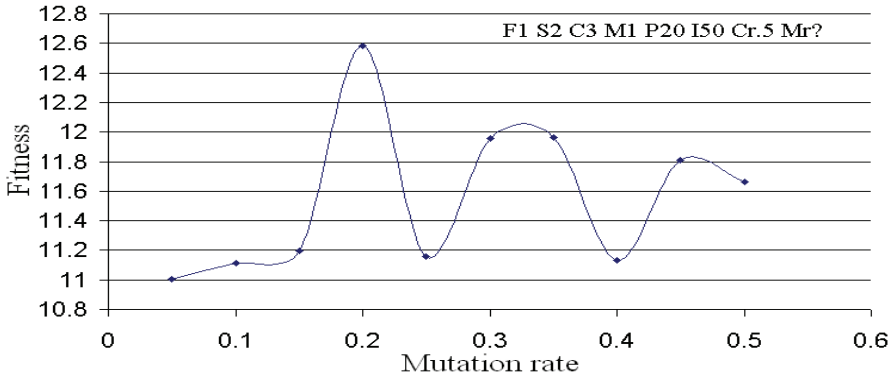


Figure 10: The mutation rate for the M1 method

5.4.6 Ranking methods

In Fig.11, three methods (Rank, Top, and Uniform) were compared with each other while under similar conditions. The “Uniform” and “Rank” methods gave a better response than the “Top” method.

One explanation could be that for the “Top” method, only a few privileged chromosomes were important. The other chromosomes lost permission to be selected because of a lower fitness relative to the first chromosome. It could be possible that these chromosomes with a low value, by intervention of the correct crossover operator, generated better children; however, this chance was eliminated for them. This happened under the conditions of the “rank” and “uniform” methods, where all of the chromosomes had the chance to be selected. In fact, some chromosomes had more chances to live and some had less chance but the chance to continue life existed for all of them.

5.4.7 Methods of selection

The three selection methods (roulette, tournament, and uniform) are compared in Fig. 12. The tournament method was chosen as the best selection method due to its lower variations, convenient slop and lowest fitness.

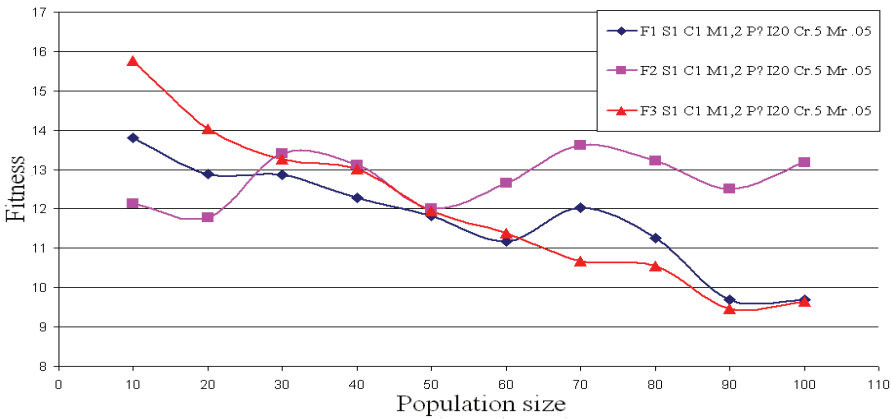


Figure 11: Obtaining the convenient scale factor method

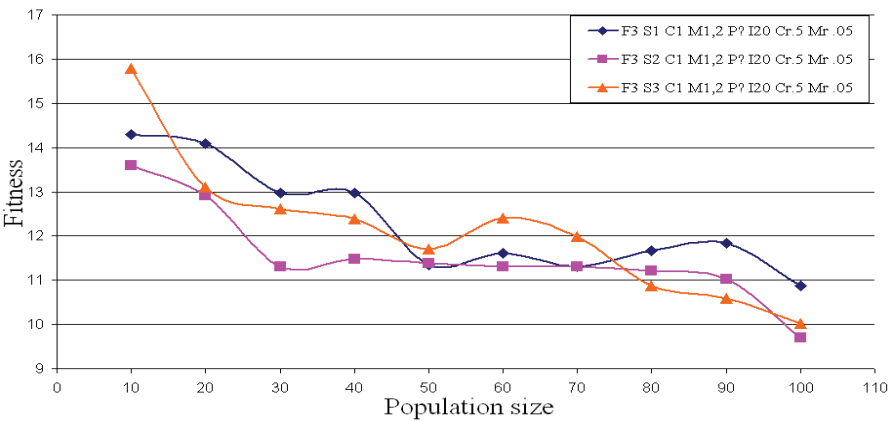


Figure 12: Obtaining the best selection method

Between the “roulette” and “tournament” methods, the “roulette” method increased the chance of selection of a population with a higher value while, at the same time, did not eliminate the chance of selection of a population with the lowest value. However, this method appeared weaker than the “tournament” method. It is noted that the scale factor, selection and crossover methods influenced the operation of each other too much. In the scale factor part, the “uniform” method gave the best response and was chosen as the scale factor method. Then, by combining the “uniform” method with the “roulette” and “tournament” methods, as by the mind of “uniform”, the whole population had an equal chance of being selected. However,

the “tournament” method compared the population two by two; thus, the selection would be carried between the whole population. After being selected by the “tournament” method, we would have a population with low fitness and also a population with high fitness. Whereas, after being selected by the “roulette” method, most of the population had a high fitness, which caused less variety between the populations. This phenomenon led to a decrease in the convergence speed.

The question remains that if all of the individuals of the population were good, should it not lead to convergence and a better fitness quantity? In fact, the existence of good individuals in a population could lead to better fitness when the best individuals in the population move to the next step every time by the elitism method. However, when the number of good individuals in the population is too high, which means that the individuals in the population have similar chromosomes, the method of crossover would not have a special influence on these elements of the population; thus, this population would not progress. However, the existence of a variety in the population eliminates this matter.

Thus, the existence of good individuals in the population was not sufficient on its own. The variety of elements in the population was also very important.

5.4.8 *Methods of crossover*

Three methods of crossover (single-point, two-point, and scatted) are compared in Fig.13. Between them, the scatted method was chosen as the best method of crossover due to its lowest quantity of fitness. We could explain it by the length of the chromosome. Since the length of the considered chromosome is high (39 characters), the methods of single-point crossover and two-point crossover were not able to correctly move the chromosomes. However, the scatted method performs the crossover operation using a chromosome with a length that is equal to the considered chromosome in our research. So the crossover operation happens better and converges quickly.

5.5 *Example of the final numerical results*

Using the obtained results from the curves of Figs. 6 to 13, we found the best state, and then we executed the program illustrated in Fig. 4. For the square-shaped sheet with unit dimensions and an applied load of $10e6N$, the weight of the structure has been computed in grams (g). The results for the first generations are illustrated in Tab.5. In Tab. 5 and 6, each of the fiber angles (+30, +45 and +60) is followed by negative fiber angles (-30, -45 and -60). Thus, the composite skins are balanced.

In the last column that corresponds to the weight of the structure, we clearly observe the scatter of the results. Finally in the hundredth generation, we obtained the

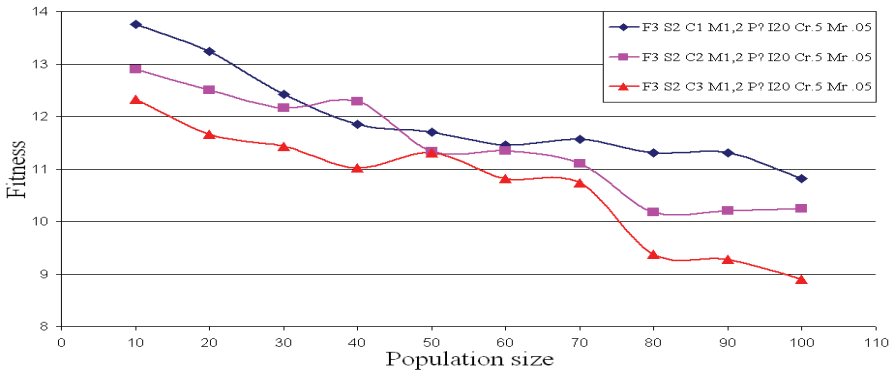


Figure 13: Obtaining a convenient method for crossover

Table 5: Results of the first generation

	Angles of fibers										Mat. (Skins)	Mat. (Core)	Height (Core)	Weight
					30	90	0	30	45	90				
1	—	—	—	—	30	90	0	30	45	90	1	3	0.005	18.36
2	—	—	—	—	0	60	90	90	30	45	0	1	0.0092	18.38
3	45	45	0	0	90	30	0	0	0	0	0	1	0.005	19.6
4	—	—	90	60	90	45	90	45	90	90	0	3	0.007	19.7
5	—	—	60	60	90	0	45	60	30	45	0	2	0.005	22
6	—	45	0	0	30	60	30	45	60	0	1	1	0.0057	22.3432
7	—	—	45	30	0	0	60	0	30	45	1	4	0.005	22.5971
8	—	30	90	30	45	90	45	60	45	30	0	2	0.0083	25.6381
9	—	0	90	0	0	0	90	90	45	45	0	4	0.005	28.7349
10	—	90	90	60	90	90	30	90	0	45	0	2	0.0111	29.3365
11	—	—	30	30	90	90	0	30	30	0	0	1	0.0181	30.0286
12	—	0	90	30	60	45	30	0	60	30	1	4	0.0063	31.5048
13	—	—	0	60	0	0	45	90	0	0	0	3	0.0187	31.6349
14	0	0	45	60	30	90	90	0	30	90	1	3	0.0098	34.581
15	—	—	45	60	0	90	60	90	90	0	1	2	0.013	35.8778
16	—	—	45	0	90	30	0	90	0	0	0	3	0.09	39.1714
17	0	0	0	30	30	90	0	0	90	90	0	3	0.0114	39.4197
18	30	90	90	0	90	60	0	0	45	60	1	2	0.086	53.419
19	90	0	90	30	0	60	60	0	60	45	0	4	0.0098	54.2476
20	45	30	0	0	0	0	30	0	60	90	0	3	0.0168	56.6476

results that are presented in Tab. 6.

The column that corresponds to the weights shows the convergence of the results, which approve our method for optimization of a sandwich structure using a genetic algorithm.

Table 6: Results of the hundredth generation

	Angles of fibers										Mat. (Skins)	Mat. (Core)	Height (Core)	Weight		
1	—	—	—	—	—	—	—	---	---	45	0	4	0.0032	8.1016		
2	—	—	—	—	—	—	—	---	---	45	0	4	0.0032	8.1016		
3	—	—	—	—	—	—	—	---	---	45	0	4	0.0032	8.1016		
4	—	—	—	—	—	—	—	---	---	45	0	4	0.0032	8.1016		
5	—	—	—	—	—	—	—	---	---	45	0	4	0.0032	8.1016		
6	—	—	—	—	—	—	—	---	---	45	0	4	0.0032	8.1016		
7	—	—	—	—	—	—	—	---	---	45	0	4	0.0032	8.1016		
8	—	—	—	—	—	—	—	---	---	45	0	4	0.0032	8.1016		
9	—	—	—	—	—	—	—	---	---	45	0	4	0.0032	8.1016		
10	—	—	—	—	—	—	—	---	---	45	0	4	0.0032	8.1016		
11	—	—	—	—	—	—	—	---	---	45	0	4	0.0032	8.1016		
12	—	—	—	—	—	—	—	---	---	45	1	4	0.0032	8.1616		
13	—	—	—	—	—	—	—	---	---	60	1	4	0.0032	8.1616		
14	—	—	—	—	—	—	—	---	---	60	1	4	0.0032	8.1616		
15	—	—	—	—	—	—	—	---	---	60	1	4	0.0035	8.8917		
16	—	—	—	—	—	—	—	---	---	90	60	1	4	0.0032	9.0216	
17	—	—	—	—	—	—	—	---	---	90	60	1	4	0.0035	9.7517	
18	—	—	—	—	—	—	—	---	---	60	90	60	1	4	0.0032	9.8816
19	—	—	—	—	—	—	—	---	---	60	90	60	1	4	0.0032	9.8816
20	—	—	—	—	—	—	—	---	---	60	90	60	1	4	0.0032	10.7416

6 Conclusion

In this research, optimization of the weight of sandwich panels was carried out using a genetic algorithm. Since our goal was to obtain the best GA method for sandwich-structure optimization, the results of this research can be expanded to the research of similar structures.

1. To create a generation with a better fitness than the previous one, choosing the number of parents and children had an important role. Regarding the obtained crossover rate, the best state happened when half of the population was composed of parents while the other half was composed of children.
2. Better covering of the search space required a convenient population size. Following the quantity of variables and the size of the search space, the population size was determined. A great population size could cause a decrease in the speed of the program's execution while a lower population size could cause it to not find the best response.
3. Increasing the generation size increased the probability of obtaining the best response. The generation size has an inverse relation to the population size.

Thus, by increasing the population size, we can reach the response with a lower generation size.

4. Choosing a mutation method required good care. For a correct mutation method choice, we should consider the length of the chromosome and the quantity of elements in the population, which should be created by the mutation method. In our research, the “uniform” method just by itself was not enough to treat the length of the chromosome; however, its combination with the “delete” method increased the speed of the treatment’s convergence.
5. Regarding the scatter in the results, the scale factor methods did not show good behavior. If good restraints were considered for the used variables, it would not be necessary to use the scale factor method. In our optimization, as the fiber orientation quantity was defined and for the skin thickness, the minimum and maximum values were considered; however, the scale factor method was not useful.
6. The manner of choosing parents is one of the most important functions of the GA, since half of the generation is composed of parents and the other half is created by the same parents with combinations of each other. If the parents are correctly chosen and have enough variety, they would cause their generation to progress. If not, they would cause elimination of their generation and deviation of other generations, which would finally cause divergence of the problem.
7. In order to cover the entire chromosome, choosing the crossover method required consideration of the length of the chromosome. For the short-length chromosomes, the single-point method and the two-point method would operate but, for the long-length chromosomes, the scattered method should be used.
8. Carrying out the sensibility analysis in the methods that should optimize the problem was very useful because it caused better convergence of the problem, decreased the program’s execution time and, at the same time, gave the best possible response.

References

Altnbach, H.; Altnbach, J. (2004): *Mechanics of Composite Structural Elements*, Springer Verlag Berlin, Heidelberg, p.468.

Aymerich, F. and Serra, M. (2006): An Ant Colony Optimization Algorithm for Stacking Sequence Design of Composite Laminates, *CMES: Computer Modeling in Engineering & Sciences*. Vol. 13, no. 1, pp. 49-66.

Gay, D.; Hoa, S.V; Tsai S.W. (2003): Composite Materials, Design and Applications, CRC Press.

Gen, M.; Cheng, R. (2000): Genetic algorithms and engineering optimization, John Wiley & Sons, Inc, p.362.

Haupt, R.L.; Haupt, S.E. (2004): Practical genetic algorithms, John Wiley & Sons, Inc, p.253.

He, Y.; Aref, A.J. (2003): An optimization design procedure for fiber reinforced polymer web core sandwich bridge deck systems. *J. Composite Structures*, vol. 60, no. 2, pp. 183–195.

Huang, S.J. and Chiu, S.W. (2008): Modeling of Structural Sandwich Plates with 'Trough-the-Thickness' Inserts: Five Layer Theory, *CMES: Computer Modeling in Engineering & Sciences*, vol.34, no.1, pp.1-32.

Hyer, M.W. (1998): Stress Analysis of Fiber Reinforced Composite Materials, McGraw Hill, p.352.

Juan, Z., Shuyao, L., Yuanbo, X. and Guangyao, L. (2008): A Topology Optimization Design for Continuum Structure Based on the Meshless Numerical Technique, *CMES: Computer Modeling in Engineering & Sciences*, vol.34, no.2, pp.137-154.

Kam, T.Y.; Lai, F.M.; Chao, T.M. (1999): Optimum design of laminated composite foam filled sandwich plates subjected to strength constraint. *J. Solids and Structures*, vol. 36, no. 19, pp. 2865-2889.

Kant, T.; Swaminathan, K. (2002): Analytical solutions for the static analysis of laminated composite and sandwich plates based on a higher order refined theory. *J. Composite Structures*, vol.60, no. 4, pp. 329–344.

Kipouros, T., Jaeggi, D.M., Dawes, W.N., Parks, G.T., Savill, A.M. and Clarkson, P.J. (2008): Insight into High-quality Aerodynamic Design Spaces through Multi-objective Optimization, *CMES: Computer Modeling in Engineering & Sciences*, vol.37, no.1, pp.1-44.

de Lacerda, L.A. and da Silva, J.M. (2006): A Dual BEM Genetic Algorithm Scheme for the Identification of Polarization Curves of Buried Slender Structures, *CMES: Computer Modeling in Engineering & Sciences*. Vol. 14, no. 3, pp. 153-160.

Li, S. and Atluri S.N. (2008a): Topology-optimization of Structure Based on the MLPG Mixed Collocation Method, *CMES: Computer Modeling in Engineering &*

Sciences, vol.29, no.1, pp.61-74.

Li, S. and Atluri S.N. (2008b): The MLPG Mixed Collocation Method for Material Orientation and Topology Optimization of Anisotropic Solid and Structures, *CMES: Computer Modeling in Engineering & Sciences*, vol.30, no.1, pp.37-56.

Narayana Naik, G.; Gopalakrishnan, S.; Ganguli R. (2008): Design optimization of composites using genetic algorithms and failure criterion. *J. Composite Structures*, vol. 83, no. 4, pp. 354-367.

Oishi, A. and Yoshimura, S. (2008): Genetic Approaches to Iteration-free Local Contact Search, *CMES: Computer Modeling in Engineering & Sciences*, vol.28, no.2, pp.127-146.

Pahr, D.H. and Rammerstorfer, F.G. (2006): Buckling of Honeycomb Sandwiches: Periodic Finite Element Considerations, *CMES: Computer Modeling in Engineering & Sciences*. Vol. 12, no. 3, pp. 229-242.

Park, J.H.; Hawang, J.H.; Lee, C.S.; Hwang, W. (2001): Stacking sequence design of composite laminates for maximum strength using genetic algorithms. *J. Composite Structures*, vol.52, no. 21, pp. 217-231.

Perko, J. and Sarler, B. (2007): Weight Function Shape Parameter Optimization in Meshless Methods for Non-uniform Grids, *CMES: Computer Modeling in Engineering & Sciences*, vol.19, no.1, pp.55-68.

Peters, S.T. (1998): Hand book of composites, second edition, Chapman & Hall.

Rajasekaran, S.; Vijayalakshmpai, G.A. (2005): Neural Networks, Fuzzy Logic and Algorithms Synthesis and Applications. Prentice Hall of India, New Delhi, p.439.

Sharnappa, Ganesan, N. and Sethuraman, R. (2007): Buckling and Free Vibrations of Sandwich General shells of Revolution with Composite facings and Viscoelastic core under Thermal Environment using Semi-analytical Method, *CMES: Computer Modeling in Engineering & Sciences*, vol.18, no.2, pp.121-144.

Sinha, S. and Ch., P. (2008): Optimization of Industrial Fluid Catalytic Cracking Unit Having Five Lump Kinetic Scheme using Genetic Algorithm, *CMES: Computer Modeling in Engineering & Sciences*, vol.32, no.2, pp.85-101.

Tan, X.H.; Soh, A.K. (2007): Multi-objective optimization of the sandwich panels with prismatic cores using genetic algorithms. *J. Solids and Structures*, vol. 44, no. 17, pp. 5466- 5480.

Venkataraman, S.; Haftka, R.T. (1999): Optimization of Composite Panels—A Review, Proceedings of the 14th Annual Technical Conference of the American Society of Composites, Sep. 27- 29, Dayton, OH, p. 419-429.

Vinson, J.R. (1999): The behavior of sandwich structures of isotropic and com-

posite material. Technomic publishing company, Inc, p.363.

Vinson, J.R.; Sierakowski, R.L. (1987): The behavior of structures composed of composite material, Kluwer Academic Publisher, Dordrecht, p.323.

Walker, M.; Smith, R.E. (2003): A technique for the multi objective optimization of laminated composite structures using genetic algorithms and finite element analysis. *J. Composite Structures*, vol. 32, no. 1, pp. 123–128.

Wang, S.Y., Lim, K.M., Khoo, B.C. and Wang, M.Y. (2007): An Unconditionally Time-Stable Level Set Method and Its Application to Shape and Topology Optimization, *CMES: Computer Modeling in Engineering & Sciences*, vol.21, no.1, pp.1-40.

Zozulya, V.V. (2009): Variational formulation and Nonsmooth Optimization Algorithms in Elastostatic Contact Problems for Cracked Body, *CMES: Computer Modeling in Engineering & Sciences*, vol.42, no.3, pp.187-215.